Multilevel quality-guided phase unwrapping algorithm for real-time three-dimensional shape reconstruction

Song Zhang, Xiaolin Li, and Shing-Tung Yau

A multilevel quality-guided phase unwrapping algorithm for real-time 3D shape measurement is presented. The quality map is generated from the gradient of the phase map. Multilevel thresholds are used to unwrap the phase level by level. Within the data points in each level, a fast scan-line algorithm is employed. The processing time of this algorithm is approximately 18.3 ms for an image size of 640 × 480 pixels in an ordinary computer. We demonstrate that this algorithm can be implemented into our real-time 3D shape measurement system for real-time 3D reconstruction. Experiments show that this algorithm improves the previous scan-line phase unwrapping algorithm significantly although it reduces its processing speed slightly.

OCIS codes: 100.6850, 120.5050, 120.2650.

1. Introduction

With the development of digital technology, real-time 3D shape measurement is increasingly important in many fields. The 3D shape measurement system using digital fringe projection and various phase-shifting methods has become more and more popular.[1–4] Zhang and Huang[5] recently developed a system that was able to do real-time 3D shape acquisition, reconstruction, and display at a speed of up to 40 frames/s using a digital fringe projection and a fast three-step phase-shifting method. The phase unwrapping method used in this system was a scan-line algorithm that allowed real-time performance. However, this simple scan-line phase unwrapping algorithm encounters significant problems when the phase map has bad quality or noise, for example. To improve the performance of the system, we are trying to develop a better phase unwrapping algorithm for real-time 3D reconstruction.

For a 3D shape measurement system using a phase-shifting-based method, the phase obtained from fringe images normally ranges from 0 to 2π. If multiple fringes are used, phase discontinuities occur every time the phase changes by 2π. Phase unwrapping aims to unwrap or integrate the phase along a path counting the 2π discontinuities. The key to reliable phase unwrapping is the ability to accurately detect the 2π jumps. However, for complex geometric surfaces, noisy images, and sharp changing surfaces, the phase-unwrapping procedure is usually difficult.[6] Different phase unwrapping algorithms have been developed to improve the robustness of the phase-unwrapping process, including the branch-cut algorithms,[7–11] the discontinuity minimization algorithm,[12] the L^p-norm algorithm,[13] the region-growing algorithm,[14,15] the agglomerative-clustering-based approach,[16] and the least-squares algorithms.[17] However, they are generally too slow for high-resolution, real-time 3D shape reconstruction application. Huntley and Salder[18] proposed a temporal phase unwrapping algorithm that was able to unwrap the phase pixel by pixel without considering the neighboring pixels. It was able to unwrap the phase map with isolated patches.[19] However, it required more than one phase map with different fringe pitch numbers, which is not desirable for our real-time system.

Quality-guided phase unwrapping algorithms unwrap the phase by using a quality map to guide the phase unwrapping path. The unwrapping process starts from the highest quality point and continues to the lower quality ones until it finishes. The quality map is usually constructed based on the first or the second difference between a value and its neighboring pixels. A number of methods have been proposed.[20–26] Although some unwrapping errors still remain undetected and propagate in a manner that depends on the

S. Zhang (szhang@fas.harvard.edu) and S.-T. Yau are with the Department of Mathematics, Harvard University, Cambridge, Massachusetts 02138. X. Li is with Geometrics Informatics Incorporated, Somerville, Massachusetts 02143.

Received 12 July 2006; revised 30 August 2006; accepted 1 September 2006; posted 7 September 2006 (Doc. ID 72940); published 15 December 2006.

0003-6935/06/010050-08$15.00/0

chosen path, these algorithms are surprisingly robust in practice.[6] However, conventional algorithms involve a time-consuming point-by-point sorting that makes it difficult to obtain real-time performance. Our experiments found that it took more than 500 ms to reconstruct one frame with an image size of 640 × 480 pixels with an ordinary personal computer (PC). By contrast, the fast scan-line algorithm was able to do phase unwrapping rapidly. If the advantages of both algorithms are combined, the processing speed of the quality-guided phase unwrapping algorithm will be boosted, and the robustness of the fast algorithm will be improved. In this research we propose such an algorithm for real-time 3D shape measurement that is designed for single connected phase maps that do not contain isolated areas of phase maps. The quality map is generated from the gradient of the phase map, then quantized into multilevels. In each level, a scan-line algorithm is applied for unwrapping. Our experiments demonstrated that the phase unwrapping time for a three-level algorithm took only 18.3 ms for one frame, and more than 99% real-time acquired facial data with normal expressions could be unwrapped correctly. We also implemented this phase unwrapping algorithm into our real-time 3D shape measurement system to demonstrate its real-time performance.

In Section 2 we explain the proposed phase unwrapping algorithm. In Section 3 we show the experimental results, and we summarize the paper in Section 4.

2. Algorithm

A. Quality Map Generation

The quality map is critical for a quality-guided phase unwrapping algorithm; the success or failure of a phase unwrapping algorithm seems to hinge on the availability of a good quality map.[6] We use two quality maps: the data modulation map and the gradient-based quality map.

1. *Quality Map 1: Removal of Background*

For a phase-shifting-based 3D shape measurement, the intensities of the fringe images can be written as

$$I_i(x, y) = I'(x, y) + I''(x, y)\cos[\phi(x, y) + \delta_i], \quad (1)$$

where $I'(x, y)$ is the average intensity, $I''(x, y)$ is the intensity modulation, $\phi(x, y)$ is the phase to be determined, and δ_i is the phase shift. Data modulation

$$\gamma(x, y) = I''(x, y)/I'(x, y) \quad (2)$$

represents the quality of the data point with 1 being the best. We found that for our system data modulation was a good quality map to remove the background of the image. Therefore data modulation is used as the first quality map for background masking.

In this research, we used a three-step phase shifting algorithm with a phase shift of $2\pi/3$. That is, $\delta_1 = -2\pi/3$, $\delta_2 = 0$, $\delta_3 = 2\pi/3$. The phase and the data modulation are

$$\phi(x, y) = \tan^{-1}\left\{\sqrt{3}\,\frac{I_1 - I_3}{2I_2 - I_1 - I_3}\right\}, \quad (3)$$

$$\gamma(x, y) = \frac{\sqrt{3(I_1 - I_3)^2 + (2I_2 - I_1 - I_3)^2}}{I_1 + I_2 + I_3}, \quad (4)$$

respectively.

2. *Quality Map 2: Guide Phase Unwrapping Path*

The other quality map used for phase unwrapping is a maximum phase gradient map that guides the phase-unwrapping path, which is defined as

$$Q(i, j) = \max\{\Delta_{i,j}{}^x, \Delta_{i,j}{}^y\} \quad \text{with } Q(i, j) \in [0, 1), \quad (5)$$

where $\Delta_{i,j}{}^x$ and $\Delta_{i,j}{}^y$ are the maximum values of the partial derivatives of the phase in the x and y directions, respectively,

$$\Delta_{i,j}{}^x = \max\{|\mathbf{W}\{\psi(i, j) - \psi(i, j-1)\}|, |\mathbf{W}\{\psi(i, j+1) - \psi(i, j)\}|\},$$

$$\Delta_{i,j}{}^y = \max\{|\mathbf{W}\{\psi(i, j) - \psi(i-1, j)\}|, |\mathbf{W}\{\psi(i+1, j) - \psi(i, j)\}|\},$$

where $\psi = \phi/(2\pi)$ is the normalized wrapped phase ϕ in Eq. (3) whose value ranges from 0 to 1. $\mathbf{W}$ is an operator that estimates the true gradient by wrapping the differences of the wrapped phase. For example, $\mathbf{W}\{0.3 - (-0.5)\} = -0.2$, $\mathbf{W}\{0.3 - (-0.1)\} = 0.4$. It should be noted that the larger the value of the quality map $Q(i, j)$ in Eq. (5), the worse the data quality; it is actually a reverse quality map.

B. Quality Map Quantization

The quality map Q in Eq. (5) is assumed to be a normal distribution after applying data modulation masking, with the mean value being $\bar{Q} = \sum_{i=1}^{N}\sum_{j=1}^{M} Q(i, j)/MN$, the standard deviation $\sigma = \sum_{i=1}^{N}\sum_{j=1}^{M}\sqrt{(Q(i, j) - \bar{Q})^2}/MN$. Here the image resolution is $M \times N$. A threshold is first chosen to divide the data into two parts, the one with higher priority to be processed and the other to be postponed for later processing. In this research, the starting quality value was found to be $th_s = \bar{Q}$. That is, the data points set $\{(i, j)|Q(i, j) < th_s\}$ must be processed in the first round. This set forms the first level (level 1). For the nth level, the threshold value is $s = th_s + 2^{(n-1)}\sigma$. The last level will unwrap the remaining points.

For the phase data acquired by our real-time 3D shape measurement system,[27] after masking the background with data modulation, more than 80% of the data points are in level 1. This is because this system uses the digital fringe projection method, and the data quality is normally good. We found that the three-level algorithm is sufficient for our system. It

should be noted that for the data acquired by our system, the more levels used, the slower the processing speed achieved, and the better the quality obtained. The extreme case of this algorithm is the conventional quality-guided phase unwrapping algorithm (which will be discussed in Subsection 2.D), in which each time there is only one pixel with a next lower quality value to proceed.

C. Scan-Line Algorithm

The scan-line algorithm used in this research is as follows. The process starts from one good point (this point is not regarded as background and has a data modulation value larger than 0.7) near the center of the image (x_0, y_0). After images are divided into four patches by the horizontal and vertical lines through the start point, each patch is unwrapped by the scan-line method. In this scan-line method, one horizontal scan-line scans from the start point to the image border. Then the scan-line advances vertically from the start point to the image border to scan another row. The neighbors (x_n, y_n) of one scanned point (x, y) can be divided into two groups: the neighbors that faced the start point, namely, the neighbors that have a smaller x or y distance to the start point than the scanned point (i.e., $|x_n - x_0| <= |x - x_0|$ and $|y_n - y_0| <= |y - y_0|$); and the neighbors that faced the border, i.e., the neighbors that have a larger x or y distance to the start point than the scanned point (i.e., $|x_n - x_0| > |x - x_0|$ or $|y_n - y_0| > |y - y_0|$). If at least one of its neighbors that faced the start point is unwrapped, a point will be unwrapped and marked as unwrapped. This point with no unwrapped neighbor facing the start point, but with at least one valid neighbor facing the border, will be pushed to the stack. After all points in a patch are scanned, the points in the stack will be popped one by one in reverse order. The popped point with at least one unwrapped neighbor facing the border will be unwrapped, while other points are abandoned. The merit of this method is that each point is scanned only once while it has two chances to be unwrapped. Therefore it results in better unwrapping results. Since this algorithm is based on line scanning, it even performs faster than the flood-fill algorithm. The schematic is shown in Fig. 1.

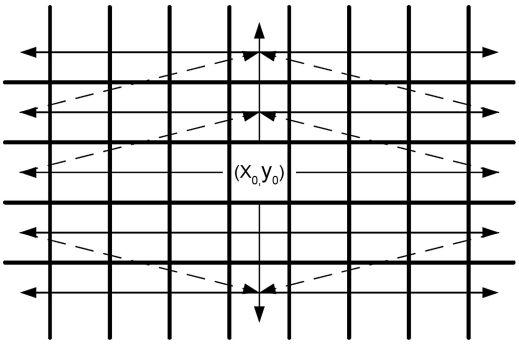

Fig. 1. Schematic of the scan-line phase unwrapping algorithm.

D. Conventional Variance Quality-Guided Algorithm

The phase derivative variance is defined by the equation

$$Z_{m,n} = \frac{\sqrt{\sum\left(\frac{\partial\psi(i,j)}{x} - \overline{\frac{\partial\psi(i,j)}{x}}\right)^2} + \sqrt{\sum\left(\frac{\partial\psi(i,j)}{y} - \overline{\frac{\partial\psi(i,j)}{y}}\right)^2}}{k^2}, \tag{6}$$

where for each sum the indices (i, j) range over the $k \times k$ window centered at the pixel (m, n). $\overline{\partial\psi(i,j)/x}$ and $\overline{\partial\psi(i,j)/y}$ are the averages of these partial derivatives in the $k \times k$ windows. Thus this equation is a root-mean-square measure of the variances of the partial derivatives in the x and y directions.

The quality guided-path-following algorithm is essentially the flood-fill algorithm as discussed in Ref. 6 in which the order of fill is determined by the quality map.

The algorithm operates as follows: A starting pixel with a high-quality value is selected and its four neighbors are examined. These neighbors are unwrapped and stored in a list called the adjoin list. The algorithm then proceeds iteratively as follows: The pixel on the list with the highest-quality value is removed from the list, and its four neighbors are unwrapped and placed in the list. (The pixels are sorted and stored in the list in the order of their quality values.) If its neighbor has already been unwrapped, it is not placed in the list. The iterative process of removing the highest-quality pixel from the list, unwrapping its four neighbors and inserting them in the list continues until all the pixels have been unwrapped.

3. Experiments

To show how this phase unwrapping algorithm works, we processed real fringe images acquired by our 3D shape measurement system. The first row in Fig. 2 shows phase-stepped three-fringe images. The image resolution is 640 × 480 pixels. The phase shift we used is 120°. Figure 2(d) shows the phase map whose value ranges from 0 to 2π. Figure 2(e) shows the data modulation map of the fringe images; from black to white, the values range from 0 to 1. Based on

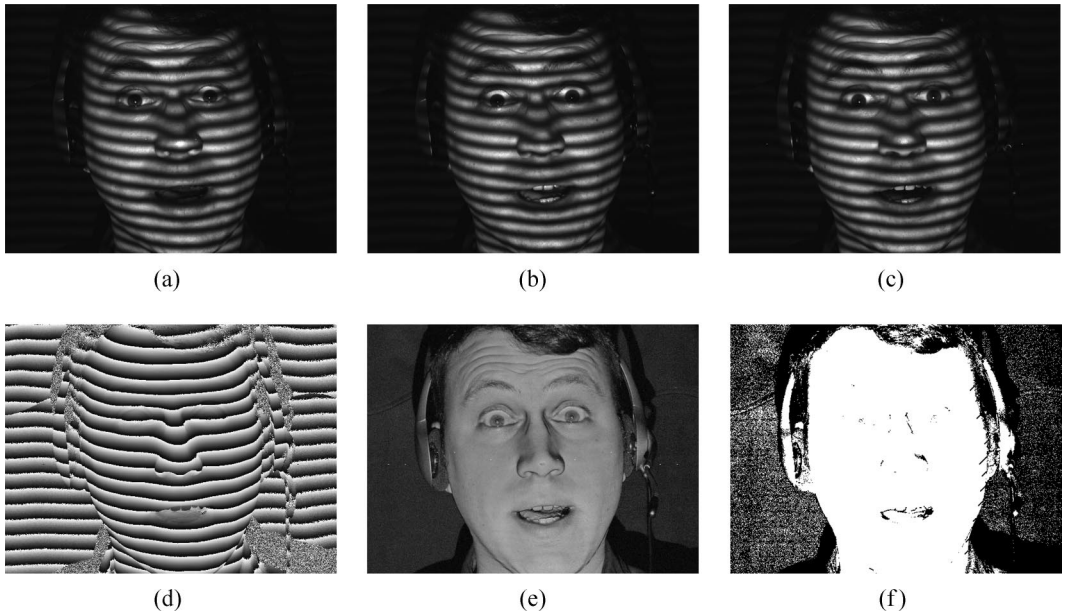

Fig. 2. Example of the data for testing our phase unwrapping algorithm. (a) $I1(-2\pi/3)$, (b) $I2(0)$, (c) $I3(2\pi/3)$, (d) wrapped phase map, (e) data modulation quality map with the white being 1.0 in value, (f) good data points after removing the background by using a threshold of gamma map (0.25), white denotes the good points and black denotes the background points.

the data modulation values obtained, we applied a threshold of 0.25 to remove the background. After having applied this threshold, we generated a mask for future processing. The mask map is shown in Fig. 2(f) with the dark points as the background.

Figure 3 demonstrates the procedures of this phase unwrapping algorithm. Once the mask map was obtained as shown in Fig. 2(f), one large connected patch was found. We considered only one single connected patch because our real-time system was able to obtain the absolute coordinates for only one single patch. For this connected patch, the quality map was computed by using Eq. (5). The quality map is shown in Fig. 3(b). The histograph of the quality map is shown in Fig. 3(c). The standard deviation of these points is 0.036, and the mean value is 0.039. Hence the first level threshold is chosen as 0.039. The second level threshold is $0.039 + 0.036 = 0.075$. Since a three-level algorithm is used, the third step unwraps the remaining points.

Figure 4 shows the unwrapped points and geometry. The first row shows the points we unwrapped after each step, which are represented as white. After phase unwrapping, the phase map was obtained, and the geometry could then be extracted, as shown in the second row. In this research, the system was calibrated by using the method proposed by Zhang and Huang.[28] It should be noted that in each level the unwrapping algorithm processed the single connected patch only to boost the efficiency. Those isolated points were postponed to the next step.

Figure 5 shows the comparison between the unwrapping results using three different algorithms. It clearly shows that the scan-line algorithm cannot obtain the correct geometry. Our algorithm can obtain similar geometry as the traditional variance guided phase unwrapping algorithm. The difference map is shown in Fig. 5(d). White means that the unwrapped results are different, and black means no difference. There was no difference between the results using

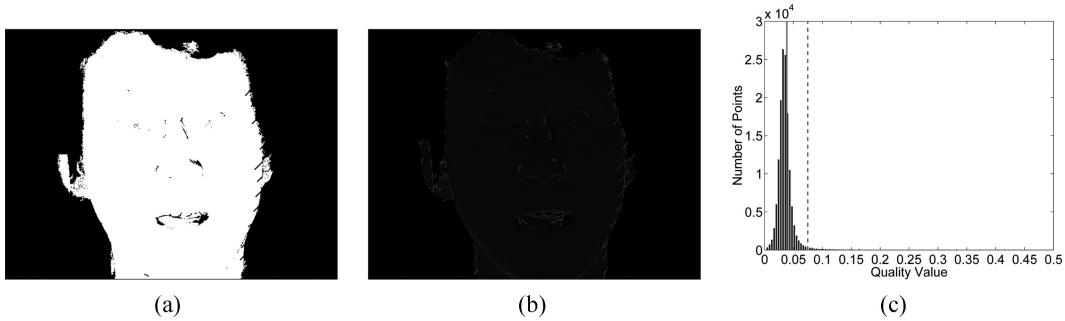

Fig. 3. Quality map and the threshold value for each level. (a) Patch of interest, the largest good connected patch; the white points are the patch of interest. (b) Quality map. (c) Histograph of the quality map. The solid line shows the mean value that determines the first threshold for the first level. The dashed line shows the threshold used for the second level. (Standard deviation δ, 0.036; mean value, 0.039.)

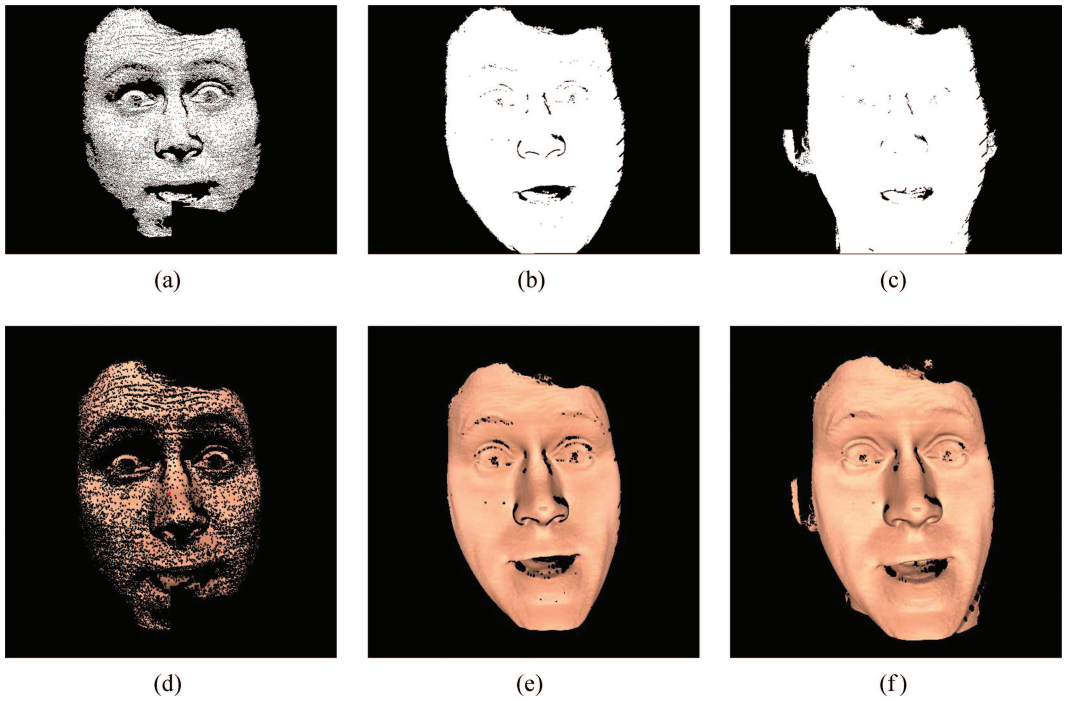

Fig. 4. (Color online) Unwrapping points after each step. The phase unwrapping starts from level 1 with the highest quality data points and unwraps these points using the scan-line algorithm, then continues to data points on a lower level until finished. (a) Unwrapping points represented as white after the first level as the first step. (b) Unwrapping points after the second step. (c) Unwrapping points when it finishes. (d) Unwrapped geometry after the first step. (e) Unwrapped geometry after the second step. (f) The final results.

the proposed algorithm and those using the conventional quality-guided phase unwrapping algorithm. In contrast, the result obtained by the fast phase unwrapping algorithm had some area different from that obtained by the conventional variance quality-guided phase unwrapping algorithm.

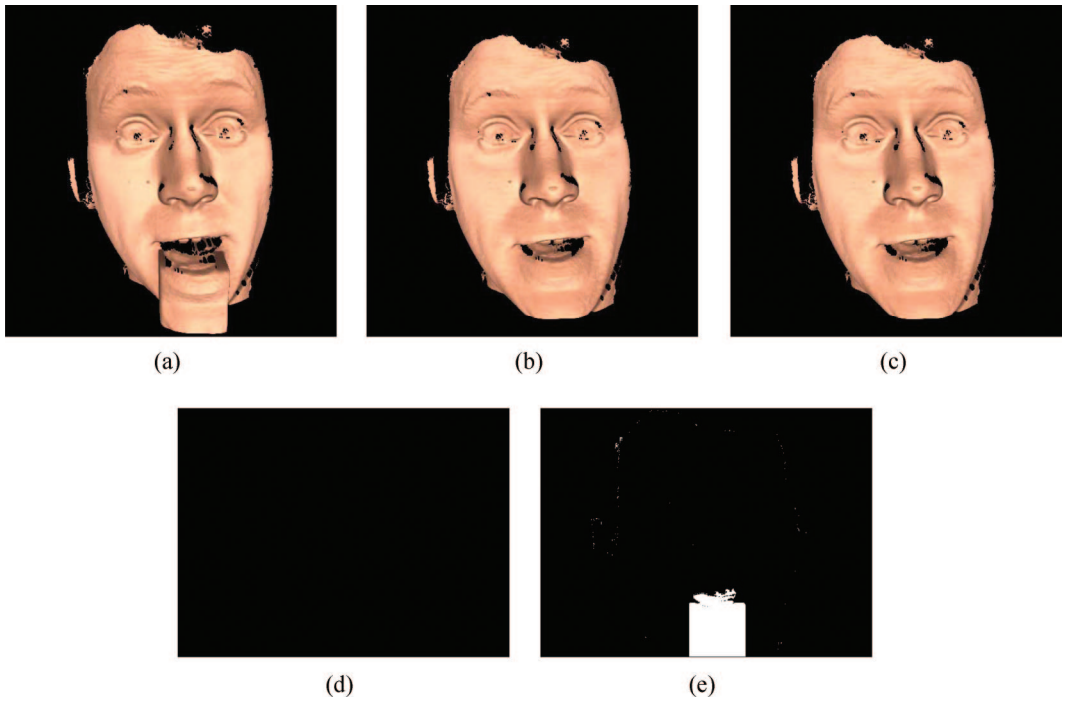

Fig. 5. (Color online) Three-dimensional reconstruction results using different phase unwrapping algorithms. (a) 3D result using fastest scan-line phase unwrapping algorithm. (b) 3D result using variance quality-guided phase unwrapping algorithm. (c) 3D result using multilevel quality-guided phase unwrapping algorithm. (d) Difference map between (b) and (c), black denotes the same and white denotes different. (e) Difference map between (a) and (b), black denotes the same and white denotes different.

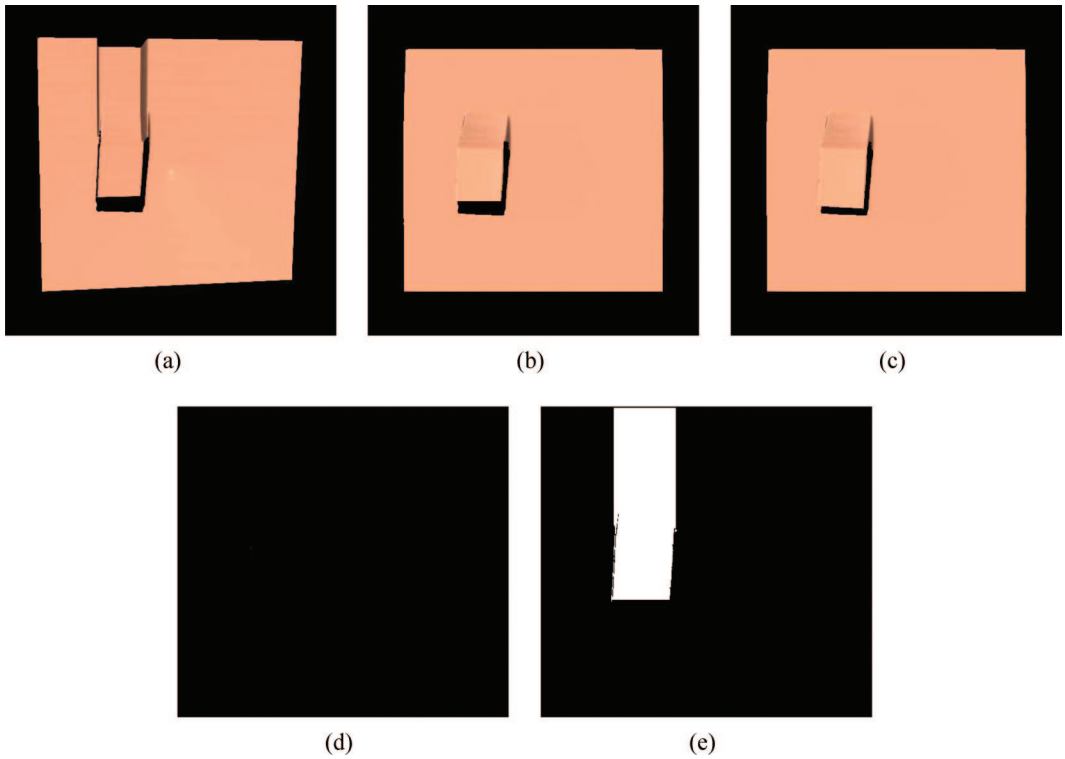

Fig. 6. (Color online) Three-dimensional shape reconstruction results for different phase unwrapping algorithms. (a) 3D result using fastest scan-line phase unwrapping algorithm. (b) 3D result using variance quality-guided phase unwrapping algorithm. (c) 3D result using multilevel quality-guided phase unwrapping algorithm. (d) Difference map between (b) and (c), black denotes the same and white denotes different. (e) Difference map between (a) and (b), black denotes the same and white denotes different.

We also tested an object with a step height on a flat board. Figure 6 shows the results using different algorithms. Again, the fastest algorithm could not correctly retrieve the geometry, while both our algorithm and the conventional quality-guided phase unwrapping algorithm could obtain the geometry correctly.

These experiments demonstrated that for the data collected by our structured light system[27] our algorithm could obtain comparable results with the traditional variance quality-guided phase unwrapping algorithm, while the speed of our algorithm was much faster. Table 1 shows the phase unwrapping time for typical face data as shown in Fig. 2. This table shows that the multilevel quality-guided phase unwrapping algorithm reduced the processing time of the traditional variance quality-guided phase unwrapping algorithm approximately 28 times.

To verify the performance of our algorithm, we tested a number of data sets acquired by our system. The comparison between the algorithms is shown in Table 2. Data sets 1–5 are typical human facial expressions. This table shows that for the scan-line algorithm, it can successfully unwrap most of the frames (more than 90%). Our multilevel quality-guided phase unwrapping algorithms failed with only a few frames, approximately 0.1%. We then captured a challenging data sequence of 1800 frames, as data set 6 in Table 2. This data set contains exaggerated and difficult facial expressions. It can be seen that the failure rate of the scan-line algorithm was more than 86%. Our phase unwrapping algorithm could successfully unwrap approximately 97%. It should be noted that, amazingly, the variance quality-guided phase unwrapping algorithm could unwrap all frames correctly. These experiments demonstrated that our proposed phase unwrapping algorithm improves

Table 1. Comparison of Phase Unwrapping Time of Different Algorithms[a]

	Path Following	Traditional Quality Guided	Multilevel
Unwrapping time (ms)	6.84	505.47	18.13

[a]The computation time was obtained with a Dell Workstation (Pentium 4, 3.4 GHz CPU, 2 Gbits memory); the image resolution is 640 × 480 pixels.

Table 2. Comparison of Phase Unwrapping Algorithms

		Number of Unsuccessful Unwrapping Frames		
Test Data	Total Frames	Path Following	Traditional Quality Guided	Multilevel
Set 1	538	56	0	0
Set 2	538	34	0	1
Set 3	538	12	0	0
Set 4	638	36	0	0
Set 5	538	19	0	2
Set 6	1800	1534	0	71

Fig. 7. (Color online) Real-time 3D reconstruction using the proposed phase unwrapping algorithm.

the scan-line phase unwrapping algorithm significantly. It takes only 18.13 msfor a typical face data. Therefore it is feasible for real-time reconstruction using the proposed algorithm. We then applied this phase unwrapping algorithm to our real-time system.[27] By employing the fast three-step phase shifting algorithm,[29] we were able to do real-time 3D shape acquisition, reconstruction, and display at 30 frames/s, similar to the system that Zhang and Huang[5] developed previously with the flood-fill phase unwrapping algorithm, but with much better results. Figure 7 shows the results during the experiments: the right image is the subject and the image on the left shows the reconstructed geometry in real time.

4. Conclusion

We presented a multilevel quality-guided phase unwrapping algorithm for real-time 3D shape measurement. It is based on a multilevel quality-guided path-flow method. The quality map was generated from the gradient of the phase map. Multilevel thresholds were used to unwrap the phase level by level. Within each level, a fast scan-line algorithm was employed. The processing time of this algorithm was approximately 18.3 ms for an image size of 640 $\times$ 480 pixels in an ordinary computer. Therefore it allows for real-time 3D shape reconstruction. Experiments showed that for the data set of normal facial expressions, the proposed algorithms could unwrap the phase correctly more than 99% of the time. For data of exaggerated facial expressions, the fast scan-line algorithm failed almost 87% of the time; the proposed algorithm could unwrap more than 97% correctly. This algorithm was successfully implemented into our real-time 3D shape measurement system, and we were able to acquire, reconstruct, and display the 3D geometry at 30 frames/s with an ordinary computer.

It should be noted that the choice of threshold is critical to correctly unwrap complex objects. The thresholds for this three-level algorithm work satisfactorily for the facial data. We found that for data set 6 in Table 2, the unsuccessfully unwrapped frames could all be correctly unwrapped by changing the thresholds slightly. A better criterion for setting the thresholds for each level might be needed to improve the robustness of the algorithm.

The authors thank Xiaomei Hao and Dale Royer for serving as models for testing our system, and thank the team at Geometric Informatics Inc. for their support. This work was performed at Geometric Informatics Inc. and funded by the Advanced Technology Program (ATP) of the National Institute of Standards and Technology (NIST).

References

1. P. S. Huang, Q. Hu, F. Jin, and F. P. Chiang, "Color-encoded digital fringe projection technique for high-speed three-dimensional surface contouring," Opt. Eng. **38,** 1065–1071 (1999).
2. P. S. Huang, C. Zhang, and F.-P. Chiang, "High-speed 3D shape measurement based on digital fringe projection," Opt. Eng. **42,** 163–168 (2003).
3. L. Kinell, "Spatiotemporal approach for real-time absolute shape measurements by use of projected fringes," Appl. Opt. **43,** 3018–3027 (2004).
4. J. Pan, P. S. Huang, and F.-P. Chiang, "Color phase-shifting technique for three-dimensional shape measurement," Opt. Eng. **45,** 013602–1–9 (2006).
5. S. Zhang and P. S. Huang, "High-resolution, real-time 3D shape measurement," Opt. Eng., to be published; http://math.harvard.edu/~songzhang/publications/realtime.pdf.
6. D. C. Ghiglia and M. D. Pritt, *Two-Dimensional Phase Unwrapping: Theory, Algorithms, and Software* (Wiley, 1998).
7. J. M. Huntley, "Noise-immune phase unwrapping algorithm," Appl. Opt. **28,** 3268–3270 (1989).
8. R. M. Goldstein, H. A. Zebker, and C. L. Werner, "Two-dimensional phase unwrapping," Radio Sci. **23,** 713–720 (1988).
9. R. Cusack, J. M. Huntley, and H. T. Goldrein, "Improved noise-immune phase unwrapping algorithm," Appl. Opt. **34,** 781–789 (1995).
10. J. R. Buchland, J. M. Huntley, and S. R. E. Turner, "Unwrapping noisy phase maps by use of a minimum-cost-matching algorithm," Appl. Opt. **34,** 5100–5108 (1995).
11. M. F. Salfity, P. D. Ruiz, J. M. Huntley, M. J. Graves, R. Cusack, and D. A. Beauregard, "Branch cut surface placement for unwrapping of undersampled three-dimensional phase data: application to magnetic resonance imaging arterial flow mapping," Appl. Opt. **45,** 2711–2722 (2006).
12. T. J. Flynn, "Two-dimensional phase unwrapping with minimum weighted discontinuity," J. Opt. Soc. Am. A **14,** 2692–2701 (1997).
13. D. C. Ghiglia and L. A. Romero, "Minimum L^p-norm two-dimensional phase unwrapping," J. Opt. Soc. Am. A **13,** 1–15 (1996).
14. A. Baldi, "Phase unwrapping by region growing," Appl. Opt. **42,** 2498–2505 (2003).
15. K. M. Hung and T. Yamada, "Phase unwrapping by regions using least-squares approach," Opt. Eng. **37,** 2965–2970 (1998).
16. M. A. Merráez, J. G. Boticario, M. J. Labor, and D. R. Burton, "Agglomerative clustering-based approach for two-dimensional phase unwrapping," Appl. Opt. **44,** 1129–1140 (2005).
17. J.-J. Chyou, S.-J. Chen, and Y.-K. Chen, "Two-dimensional phase unwrapping with a multichannel least-mean-square algorithm," Appl. Opt. **43,** 5655–5661 (2004).
18. J. M. Huntley and H. O. Saldner, "Temporal phase-

unwrapping algorithm for automated interferogram analysis," Appl. Opt. **32,** 3047–3052 (1993).
19. H. O. Saldner and J. M. Huntley, "Temporal phase unwrapping: application to surface profiling of discontinuous objects," Appl. Opt. **36,** 2770–2775 (1997).
20. D. J. Bone, "Fourier fringe analysis: the two-dimensional phase unwrapping problem," Appl. Opt. **30,** 3627–3632 (1991).
21. J. A. Quiroga, A. Gonzalez-Cano, and E. Bernabeu, "Phase-unwrapping algorithm based on an adaptive criterion," Appl. Opt. **34,** 2560–2563 (1995).
22. M. D. Pritt, "Phase-unwrapping by means of multigrid techniques for interferometric SAR," IEEE Trans. Geosci. Remote Sens. **34,** 728–738 (1996).
23. B. Ströbel, "Processing of interferometric phase maps as complex-valued phasor images," Appl. Opt. **35,** 2192–2198 (1996).
24. J.-L. Li, X.-Y. Su, and J.-T. Li, "Phase unwrapping algorithm based on reliability and edge detection," Opt. Eng. **36,** 1685–1690 (1997).
25. M. A. Herráez, D. R. Burton, M. J. Lalor, and M. A. Gdeisat, "Fast two-dimensional phase-unwrapping algorithm based on sorting by reliability following a noncontinuous path," Appl. Opt. **41,** 7437–7444 (2002).
26. C. Quan, C. J. Tay, L. Chen, and Y. Fu, "Spatial-fringe-modulation-based quality map for phase unwrapping," Appl. Opt. **42,** 7060–7065 (2003).
27. S. Zhang and S.-T. Yau, "High-resolution, real-time absolute coordinate measurement based on the phase-shifting method," Opt. Express **14,** 2644–2649 (2006).
28. S. Zhang and P. S. Huang, "Novel method for structured light system calibration," Opt. Eng. **45,** 083601–1–8 (2006).
29. P. S. Huang and S. Zhang, "Fast three-step phase-shifting algorithm," Appl. Opt. **45,** 5086–5091 (2006).